A SCENARIO APPROACH TO OPTIMIZE RESOURCES DISPATCH AND MARKET BIDDING STRATEGY OF A MULTI-ENERGY SYSTEM

Alberto Vannoni[1]*, Edoardo Corsetti[1]

[1]Ricerca sul Sistema Energetico, Department of Materials and Generation Technologies, Milan, Italy

*alberto.vannoni@rse-web.it

ABSTRACT

As global energy systems move toward sustainability, the integration of diverse energy sources into multi-energy systems is crucial for increasing system flexibility and integrating renewable energy to meet energy demands traditionally relied on fossil fuels. Optimizing these systems is essential for efficient electricity market participation, storage management, and satisfaction of local demand. While traditional linear programming algorithms are widely used, they are limited; more accurate techniques such as quadratic, conic, or nonlinear programming are used to handle more complex functions. However, these algorithms rely on deterministic input variables and can lead to suboptimal scheduling when run one day ahead using uncertain forecasts. This paper aims to quantify the impact of uncertainties in electricity price and heat demand and proposes a scenario approach for robust optimization of electricity market bidding strategies. The methodology involves running multiple deterministic optimizations, solving each unit commitment problem deterministically, and translating it into a set of bids for the electricity market. Market clearing is then simulated in each scenario to determine the accepted bids and the actual cost of each optimal solution. The best bidding strategy is determined based on expected actual costs. As a case study, a plant in the district heating network of East Milan is considered. It employs different conversion technologies such as power-to-heat, gas-to-heat, cogeneration, and thermal storage. The results highlight the intrinsic robustness of the proposed bidding methodology in ensuring the resilience of multi-energy systems in the context of dynamic markets and evolving energy landscapes.

1 INTRODUCTION

In the ongoing transition towards sustainability, the integration of diverse energy carriers by means of Multi-Energy Systems (MES) emerges as a pivotal strategy to enhance system flexibility, reliability, and resilience. Multi-Energy Systems represent a holistic approach to energy management, where various energy carriers such as electricity, heat, and gas are integrated, coordinated, and optimized to meet diverse energy demands efficiently [1].

The significance of Multi-Energy Systems lies in their ability to address the inherent intermittency and variability of renewable energy sources, such as wind and solar power, by leveraging complementary energy carriers and storage technologies[2,3]. By intelligently coupling different energy vectors, Multi-Energy Systems offer a promising pathway toward achieving higher shares of renewable energy penetration while ensuring grid stability and energy security [4]. Moreover, the synergy among different carriers may support the decarbonization of “hard-to-abate” final uses (as the demand for high-temperature process heat in industry, and the transport on long distances through maritime and aviation)[5].

Sector coupling can be implemented by connecting two or more energy carriers through specific technologies acting as an energy converter, different technologies can be classified according to the involved carriers. Power-to-gas mainly involves electrolysers to split water into oxygen and hydrogen. Hydrogen represents an energy carrier itself, but its storage is expensive therefore other chemicals that serve as hydrogen carriers must be considered. At least two options can be identified: carbon and nitrogen chemistries [6,7]. Electric vehicles represent the coupling between automotive energy

https://doi.org/10.52202/077185-0212

consumption, traditionally relying on fossil fuels, and the power sector [8]. Moreover, vehicle-to-grid technologies allow supporting the electricity grid with the provision of ancillary services [9]. Power-to-heat technologies consist of heat pumps (HPs) and electric heaters. Heat is demanded for space heating and hot water at low-temperature and from industrial processes up to notable temperatures. However, this is a relevant sector since the demand for heat represents almost half of the total final energy consumption and 38% of energy-related CO_2 [10]. The coupling to the electrical sector offers unique opportunities for decarbonization, especially through heat pumps that in many markets are becoming competitive for gas boilers replacement [11]. However, high supply temperatures negatively impact both efficiency and capital cost and the readiness of this technology beyond 100-120°C is controversial [12]. Other key technologies are combined heat and power (CHP) generators, typically gas turbines, operating through open cycles or combined cycles, or internal combustion engines.

The awareness of the strategic importance of heat integration is proven by the investments in relevant infrastructure to deliver the heat, centrally generated by coupled technologies, to the final users. District heating is today a mature technology and the progressive decrease in supply temperature increases the energy efficiency and expand the pool of connectable technologies. The state-of-the-art 4th and 5th generations typically include CHP, HPs, renewable heat generators such as biomass boilers and solar thermal collectors, recovery of waste heat, and network exploitation both for heating and cooling purposes [13].

However, the economics and emissions reduction potential of MES rely on accurate scheduling and real-time management [14]. Thus, uncertainties inherent in energy markets and local energy demand forecasts pose significant challenges [15]. Inaccurate predictions of electricity prices and heat demand can lead to suboptimal decisions, resulting in increased operational costs and reduced efficiency. The impact of poor forecasting is significant considering that Multi-Energy Systems typically operate in liberalized energy markets, where the programs for withdrawals and injections from and into the grid (electricity or, more rarely, gas) are defined by spot markets clearing. [16]. Deviations from the defined programs are settled a posteriori by the relative grid operators that charge the MES balancing responsible party (i.e., that subject representing the MES on the energy markets and responsible for the execution of the programs) considerable economic penalties. Bilateral contracts where the energy is traded in advance between two operators are possible both for gas and electricity but are much more a consolidated practice for trading natural gas. Due to the lower physical inertia of electrical phenomena, the balancing of the electrical grid is more severe, resulting in a stricter constraint of compliance with the defined program. Consequently, the uncertainty of energy demand (due to the stochasticity of user behavior and the local renewable energy production) and the clearing of the electricity market are the two main causes of suboptimal strategy implementation when optimizing the scheduling of MESs.

Traditional methods for Multi-Energy System optimization often rely on deterministic models, based on mathematical programming, which overlook uncertainties of real-world energy systems. To address these limitations, robust optimization and stochastic programming approaches have gained prominence. In the former, knowledge about probability distributions of uncertain parameters is not assumed, unlike stochastic programming where it is. Stochastic optimization aims to optimize the expected value of the objective function, often using two-stage approaches [15]. While in the absence of probability information, robust optimization focuses on minimizing worst-case performance. Adjustable Robust Optimization improves economic performance reducing solution conservativeness [17]. However, current approaches struggle to translate optimal scheduling into spot market bids effectively.

The proposed methodology here proposed for MES bidding strategy and scheduling optimization takes place in three steps. First, based on the forecasted values a common optimizer is executed; secondly, an algorithm is proposed to translate this program into an optimal set of bids; Finally, after the markets have been cleared, near real-time redispatch optimization is carried out to minimize costs while meeting the actual local energy demand compliantly with the grid program defined by the market.

Through the case study of a district heating network introduced in Section 2, and the methodology presented in Section 3, the impact of forecast uncertainties is assessed for heat demand and electricity price in Section 4. Finally, Section 5 demonstrates the applicability and efficacy of the proposed stochastic methodology in improving system performance and cost-effectiveness.

 https://doi.org/10.52202/077185-0212

2 THE CASE STUDY

This work examines the Canavese plant in the east-Milan District Heating Network as a case study. The plant aim is to meet hourly heat demand using two gas boilers, two heat pumps, one electric boiler, three gas-fired cogenerative internal combustion engines, and two thermal storages. It operates as a multi-energy system since it integrates heat, gas, and electricity. The gas is supplied through the gas grid with a long-term bilateral contract, therefore paid at the daily price without any constraint on the withdrawal schedule. Electricity, required for the heat pumps and electric boiler, is traded on the day-ahead spot market or generated by the CHP engines. The net balance between generation and consumption determines the grid injection/withdrawal program.

Electricity price is set by the day-ahead market in the Italian NORD bidding zone with an hourly resolution, it is assumed the MES manager has a proprietary tool to predict the price on a 48 h horizon with an associated uncertainty. This implies that the MES manager at the day-ahead market closure (i.e., 12 p.m. of day-1) can predict the price until 12 p.m. of day+1. The same time resolution and forecast term capability are assumed for the heat demand. The gas is paid at the daily national day-ahead market for natural gas, and at the electricity market gate closure, it is assumed to be certain for the following two days. Given this knowledge of future prices and demand, optimizing the bidding strategy requires implementing a rolling horizon of 36 h.

2.1 Technologies model

Each generator represents a pivotal node of the modelled Multi-Energy Systems. Indeed, the main generators feature is to link two energy carriers converting energy. Each conversion process is characterized by an efficiency rate that may depend both on the involved device and the operating load. To model each technology and allow for an effective optimization the energy consumption relative to the generic carrier x is linearized with respect to the thermal output P_{th} as in Equation (1).

$$P_x = \alpha_x + \beta_x \cdot P_{th} \quad (1)$$

Conventionally for all the carriers, the power signs are assumed positive when there is output from the generator. As a matter of example, when operating a CHP, thermal generation (positive P_{th}) is reflected in an electricity output (positive P_{el}) and gas consumption (negative P_{gas}). Gas consumption is expressed in MW, i.e., the product of the gas mass flow and the lower heating value. Moreover, every technology is associated with a cost of the start-up event and a specific variable O&M cost (including even auxiliary energy consumption from all the carriers), fixed O&M costs are not modelled since only variable ones impact the decision on the optimal schedule.

Table 1: Generation technologies main data in input to the optimization algorithm

Device	Abbre-viation	N	$P_{th\,max}$ [MW_{th}]	$P_{th\,min}$ [MW_{th}]	α_{el} [MW_{el}]	β_{el} [MW_{el}/MW_{th}]	α_{gas} [MW_{gas}]	β_{gas} [MW_{gas}/MW_{th}]	c_{SU} [€/SU]	$c_{O\&Mvar}$ [€/MW_{th}]
Gas boiler	GB	2	16.1	1	0	0	0.0192	-1.1740	0 [18]	1.17 [18]
Heat pump 1	HP1	1	14.725	7	-0.7783	-0.3334	0	0	156.53 [18]	1.80 [18]
Heat pump 2	HP2	1	3	1	-0.1366	-0.2978	0	0	31.89 [18]	2.33 [18]
Electric boiler	EB	1	10	0.3	0	-1.0050	0	0	0 [18]	0.96 [18]
Gas engine	CHP	3	4.4	2.2	0	1.1636	0	-2.4695	0 [18]	6.68 [18]
Thermal storage	STO	2	11	0.44	0	0	0	0	0 [19]	0.70 [19]

2.1.1 Gas boiler (GB) model: the two gas boilers in the Canavese plant have a maximum thermal power output of 16.1 MW_{th} while the minimum load is fixed at 1 MW_{th}. The efficiency is modelled according to the approach presented by Baldi et al. accounting for the load (i.e., the ratio between the power output and the maximum value) and the return temperature [20] but with updated coefficients provided directly by the authors. The return temperature has been assumed 60°C as the typical value of the Milan DHN.

Figure 1 shows the comparison between the adopted model of efficiency (dashed line) and the model originally proposed by Baldi [20] (squared markers). Although for the imposed return temperature there is not a great impact of load on efficiency the efficiency increases at lower load, due to the improved heat exchange between lower mass flows at fixed surface. The proposed fitting of the gas consumption well describes the real trend, even if the efficiency modelling diverges up to 1 percentage point at the minimum load, however the very low absolute power makes the error negligible looking at the gas consumption. The red vertical line highlights the minimum load limit. According to the Danish Energy Agency technology catalogue, the $c_{O\&M\,var}$ and c_{SU} for such a size boiler are assumed respectively 0 €/SU and 1.17 €/MW_{th} [18].

https://doi.org/10.52202/077185-0212

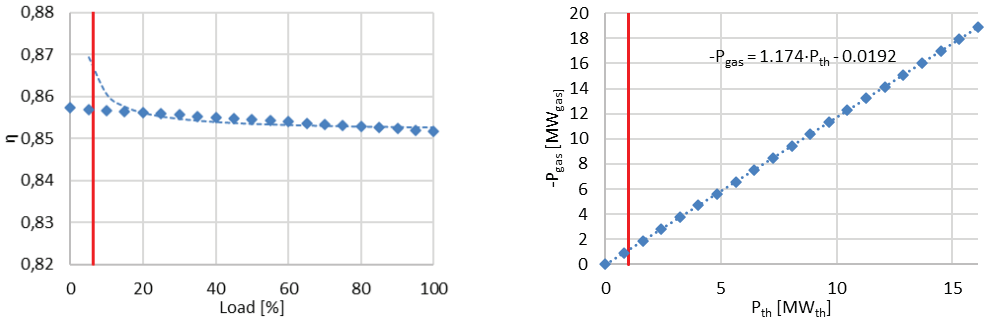

(a) (b)

Figure 1: Gas boiler efficiency and gas consumption modelling. Squared markers and the dashed lines identify the model proposed by Baldi et al [20] and that adopted in this work respectively.

2.1.2 Heat pump 1 (HP1) model: HP1 is a geothermal sourced heat pump connected to a groundwater wells system that elaborates 1000m^3/h. According to the data provided by the Original Equipment Manufacturer (OEM) the Coefficient of Performance COP is regressed against supply temperature and load as in Equation 2 where the temperature is expressed in Celsius degrees.

$$COP = 2.3378 + 0.0060 \cdot \frac{P_{th}}{P_{th_{max}}} - 0.0038 \cdot T_{supply} \quad (2)$$

The supply temperature is fixed to the value required by the Milan DHN (i.e., 85°C). In Figure 2 the blue squared marker identifies the fitting of the OEM data (Eq. 2), while the dashed line is the linear regression of the electrical consumption (i.e., -P_{el}) against the thermal output. The only original OEM datum available for the considered supply temperature is plotted by a red square. The COP varies from 2.3 at the minimum load (i.e., 50%) up to 2.6 for full-load operations. According to the Danish Energy Agency technology catalogue, the $c_{O\&M\ var}$ and c_{SU} for such a size HP are assumed respectively 156.53 €/SU and 1.8 €/MW$_{th}$ [18].

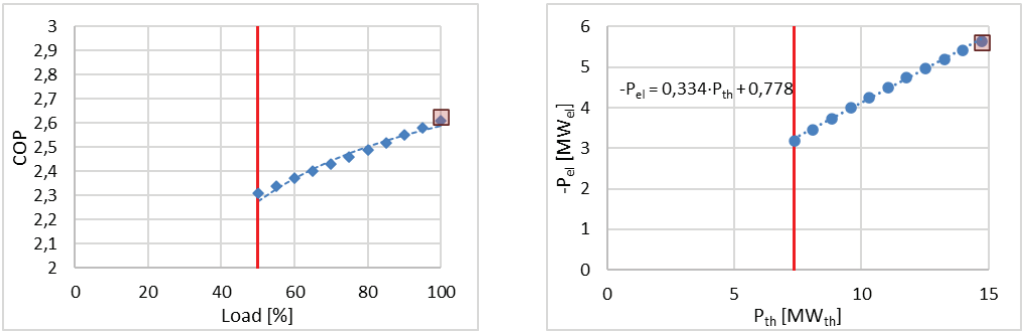

(a) (b)

Figure 2: Heat pump 1 COP and electric consumption. Blue squared markers and the dashed lines identify the fitting of OEM data and the model adopted in this work respectively.

2.1.3 Heat pump 2 (HP2) model: HP2 exploits waste heat as the lower source heat from the second stage of the intercooler of each CHP. Thus, it can be operated only if at least one CHP engine is on. Modelling of HP2 is analogous to HP1, however two datasets were available from the OEM thus both of them were used in the fitting procedure shown in Figure 3. According to the Danish Energy Agency technology catalogue, the $c_{O\&M\ var}$ and c_{SU} for such a size HP are assumed respectively 156.53 €/SU and 1.8 €/MW$_{th}$ [18].

2.1.4 Electric boiler (EB) model: The electric boiler is the most recently installed generator in the Canavese plant. Its modeling is easier because of its substantial independence of efficiency on the load with a constant value of 99.5%. Consequently, α_{el} is zero and the gas consumption is purely proportional to the thermal output. Start-up costs are null and $c_{O\&M\ var}$ is equal to 0.96 €/MW$_{th}$ [18].

https://doi.org/10.52202/077185-0212

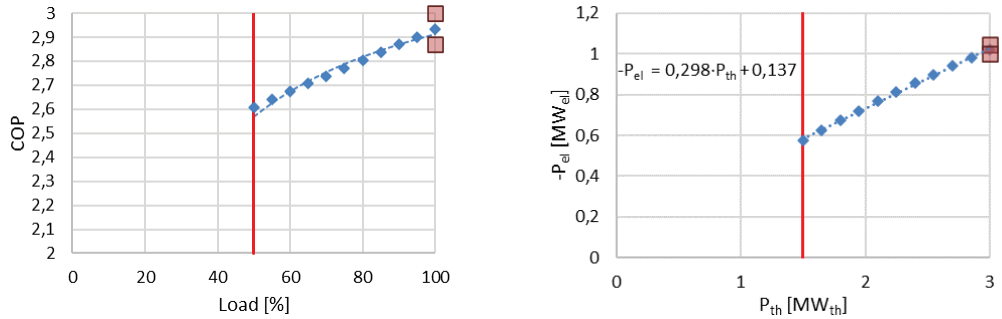

(a) (b)

Figure 3: Heat pump 2 COP and electric consumption modeling. Blue squared markers and the dashed lines identify the fitting of OEM data and the model adopted in this work respectively.

2.1.5 Gas-fired cogenerative engine (CHP) model: There are three internal combustion engines, fed by natural gas, producing both a thermal and electrical output. Therefore, it is necessary to model both the electrical and thermal efficiency. Nevertheless, varying load efficiencies are constant at 47.1% and 40.5% electrical and thermal respectively. It is therefore worth noticing that α_{el} and α_{gas} are both zero, while β_{gas} and β_{el} are negative and positive respectively indicating that a thermal output is associated with an electrical output and gas consumption. Start-up costs are null and $c_{O\&M\ var}$ is equal to 6.68 €/MW_{th} [18].

2.1.6 Thermal storage (STO) model: Finally, there are two thermal storage consisting of two water tanks of 1.000 m^3 each that, considering the DHN return (60 °C) and supply (85°C) temperatures, storage capacity is about 29 MWh_{th}. The maximum and the minimum power during charging and discharging phases are 11 and 0.44 MW respectively. Start-up costs are null and $c_{O\&M\ var}$ is equal to 0.77 €/MW_{th} [19]. Charging and discharging efficiencies, as well as the autodischarge rate over time, are neglected.

3 MES SCHEDULER AND MARKET BIDS OPTIMIZER

As shown in Figure 4, the proposed dispatch optimization procedure occurs in three steps: initial unit commitment optimization, determination of electricity market bids, and final redispatch optimization. The first step, described in Section 3.1, is based on the gas price, the forecasted heat demand, and the electricity price, it minimizes the cost of meeting the heat demand. This initial optimization provides a guess of the optimal scheduling of storage and residual load for pure generators. Residual load is then allocated to generators based on the procedure described in Subsection 3.2, generating bids for the electricity market. The market clearing determines prices and accepted bids, defining the next day's injection/withdrawal program. Finally, an optimization is performed in near real-time, similarly to step 1, but considering the actual heat demand and the constrained injection/withdrawal program.

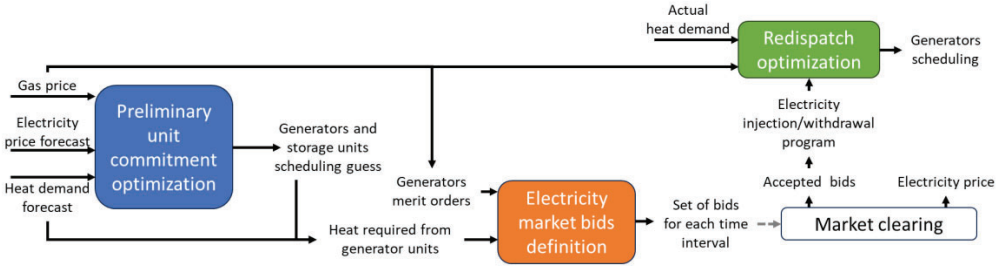

Figure 4: Three-stage optimization including the definition and submission of an optimal set of bids.

3.1 Preliminary unit commitment optimization

The definition of such a problem represents a standard in the management of Multi-Energy Systems, however here it is presented as the first of three stages of the proposed methodology. Moreover, the present subsection aims to present the specificities of the problem applied to the considered case study of Canavese plant within the East-Milan DHN. Equation 3 defines the optimization problem.

$$\min_{P_{th}} \sum_{t}^{H} \sum_{i}^{N_{units}} \left(C_{el\,i,t} + C_{gas\,i,t} + C_{O\&Mvar\,i,t} + C_{SU\,i,t} \right) \tag{3}$$

https://doi.org/10.52202/077185-0212

Where H is the number of time intervals included in the optimization horizon, N_{units} is the number of generators and storage (10 in the case study presented in Section 2). The objective function is the summation of the cost of electricity and gas consumption, the variable O&M costs, and the cost associated with any start-up event. Through a set of constraints, reported below, the terms of Equation 3 are correlated to the optimization variable $\overrightarrow{P_{th}}$.

$$C_{el_{i,t}} \geq P_{el_{i,t}} \cdot p_{el_t} = \left(\alpha_{el_i} + \beta_{el_i} \cdot P_{th_{i,t}}\right) \cdot p_{el_t} \quad \forall i \leq N_{units} \wedge \forall t \leq H \tag{4}$$

$$C_{gas_{i,t}} \geq P_{gas_{i,t}} \cdot p_{gas} = \left(\alpha_{el_i} + \beta_{el_i} \cdot P_{th_{i,t}}\right) \cdot p_{gas} \quad \forall i \leq N_{units} \wedge \forall t \leq H \tag{5}$$

$$C_{O\&Mvar_{i,t}} \geq c_{O\&Mvar_i} \cdot P_{th_{i,t}} \quad \forall i \leq N_{units} \wedge \forall t \leq H \tag{6}$$

$$C_{SU_{i,t}} \geq c_{SU_i} \cdot y_{SU_{i,t}} \quad \forall i \leq N_{units} \wedge \forall t \leq H \tag{7}$$

It is worth noticing that $C_{el_{i,t}}$ can be also negative (i.e., a profit) for those units presenting a negative β_{el}, the three CHP engines in the introduced case study. Finally, the SU costs are the product of the cost for each event for the i-th unit and the binary variable $y_{SU_{i,t}}$ that is imposed to be 1 if a start-up event subsists trough the following additional constraint.

$$y_{SU_{i,t}} \geq y_{on_{i,t}} - y_{on_{i,t-1}} \quad \forall i \leq N_{units} \wedge \forall 1 < t \leq H \tag{8}$$

$$y_{SU_{i,t}} \geq y_{on_{i,t}} - y_{0_{on_i}} \quad \forall i \leq N_{units} \wedge \forall t = 1 \tag{9}$$

$\overrightarrow{y_{on}}$ is an array of binary variables indicating if the unit i-th is on at the t-th time interval, $y_{0_{on}}$ is the initial status of the i-th unit. $y_{0_{on}}$ is set to 0 at the first day (n=1), then implementing the rolling horizon algorithm is set to $y_{on_{i,24}}$ retuned by the optimization of day n-1. Moreover, the single unit thermal output is constrained by the maximum and the minimum power.

$$y_{on_{i,t}} \cdot P_{th_{min_i}} \leq P_{th_{i,t}} \leq y_{on_{i,t}} \cdot P_{th_{max_i}} \quad \forall i \leq N_{units} - N_{STO} \wedge \forall t \leq H \tag{10}$$

Equations 10 concerns all the pure generators, therefore excluding the storage for which the thermal output $P_{th_{i,t}}$ is admitted being negative during the charging phase. To take into account this specificity new variables are introduced $P_{th_{ch}}$ and $P_{th_{disch}}$ that are non-negative real and imposed by the following set of equations to represent the positive thermal power of storage charging and discharging respectively and constrained by $P_{th_{max_s}}$ and $P_{th_{min_s}}$

$$P_{th_{s,t}} = P_{th_{ch_{s,t}}} - P_{th_{disch_{s,t}}} \quad \forall s \leq N_{STO} \wedge \forall t \leq H \tag{11}$$

$$y_{on_{N_{units}-N_{STO}+s,t}} \cdot P_{th_{min_s}} \leq P_{th_{ch_{s,t}}} \leq y_{on_{N_{units}-N_{STO}+s,t}} \cdot P_{th_{max_s}} \quad \forall s \leq N_{STO} \wedge \forall t \leq H \tag{12}$$

$$y_{on_{N_{units}-N_{STO}+s,t}} \cdot P_{th_{min_s}} \leq P_{th_{disch_{s,t}}} \leq y_{on_{N_{units}-N_{STO}+s,t}} \cdot P_{th_{max_s}} \quad \forall s \leq N_{STO} \wedge \forall t \leq H \tag{13}$$

Storages must be also constrained to not exceed the maximum and not fall below the minimum (assumed 0 in the presented case study) storage capacity.

$$E_{min_s} \leq \sum_{\tau=1}^{t} -P_{th_{s,\tau}} + E_{0_s} \leq E_{max_s} \quad \forall s \leq N_{STO} \wedge \forall t \leq H \tag{14}$$

The summation in Equation 14 represents the amount of energy stored between the time interval 1 and t adding the initial energy stored it is imposed the compliance with the storage capacity. E_{0_s} is set to 0 at the first day (n=1), then implementing the rolling horizon algorithm is set as in Equation 15 with the output returned by the optimization of day n-1.

$$E_{0_{s_n}} = \left(\sum_{\tau=1}^{24} -P_{th_{s,\tau}} + E_{0_s}\right)_{n-1} \quad \forall s \leq N_{STO} \wedge n > 1 \tag{15}$$

It is necessary to consider the specificity of HP2 that can be on only if at the least on CHP engine is on

$$y_{on_{hp2,t}} \leq \sum_{chp=1}^{N_{CHP}} y_{on_{chp,t}} \; \forall hp2 \leq N_{HP2} \wedge t \leq H \tag{16}$$

Finally, the fulfilment of the heat demand is imposed.

$$\sum_{i=1}^{N_{units}} P_{th_{i,t}} \geq HeatDemand_t \quad \forall t \leq H \tag{17}$$

https://doi.org/10.52202/077185-0212

3.2 Optimal electricity market bids generator

Each generator is characterized by an operating cost that depends on the energy consumption of gas and electricity, and so on the efficiencies associated with each carrier and unitary cost. However, commodities prices are highly mutable, especially the electricity price varies considerably on an hourly basis. Thus, the technology economic merit order (i.e., the rank from the cheapest to the most expensive generator) is variable. Assuming the gas price is known, the merit order for the technologies installed in Canavese plant depends on the electricity price as described in Table 2.

Table 2: Generation technologies main data in input to the optimization algorithm

Scenario	Condition	#1	#2	#3	#4	#5
σ=0	$p_{el} \leq p_1$	HP2	HP1	EB	GB	CHP
σ=1	$p_1 < p_{el} \leq p_2$	HP2	HP1	EB	CHP	GB
σ=2	$p_2 < p_{el} \leq p_3$	HP2	HP1	CHP	EB	GB
σ=3	$p_3 < p_{el} \leq p_4$	HP2	HP1	CHP	GB	EB
σ=4	$p_4 < p_{el} \leq p_5$	HP2	CHP	HP1	GB	EB
σ=5	$p_5 < p_{el} \leq p_6$	CHP	HP2	HP1	GB	EB
σ=6	$p_6 < p_{el} \leq p_7$	CHP_{max}	HP2	HP1	GB	EB
σ=7	$p_7 < p_{el} \leq p_8$	CHP_{max}	HP2	GB	HP1	EB
σ=8	$p_{el} > p_8$	CHP_{max}	GB	HP2	HP1	EB

The threshold values mentioned in the second column of Table 2 represent the limits on which one technology becomes cheaper than another, except for p_6 which represents the threshold beyond which it is worth operating the CHP at maximum load to sell electricity on the market independently of the heat demand fulfilment. They are assessed on the basis of rough efficiency values (independent of the load) as it follows:

$$p_1 = p_{gas} \cdot \eta_{el_{CHP}} \cdot \left(\frac{1}{\eta_{th_{CHP}}} - \frac{1}{\eta_{GB}}\right) \cong p_{gas} \cdot 0.61 \tag{18}$$

$$p_2 = p_{gas} \cdot \left(\eta_{th_{CHP}} \cdot \left(\frac{\eta_{el_{CHP}}}{\eta_{th_{CHP}}} + \frac{1}{\eta_{EB}}\right)\right)^{-1} \cong p_{gas} \cdot 1.14 \tag{19}$$

$$p_3 = p_{gas} \cdot \frac{\eta_{EB}}{\eta_{GB}} \cong p_{gas} \cdot 1.16 \tag{20}$$

$$p_4 = p_{gas} \cdot \left(\eta_{th_{CHP}} \cdot \left(\frac{\eta_{el_{CHP}}}{\eta_{th_{CHP}}} + \frac{1}{COP_{HP1}}\right)\right)^{-1} \cong p_{gas} \cdot 1.59 \tag{21}$$

$$p_5 = p_{gas} \cdot \left(\eta_{th_{CHP}} \cdot \left(\frac{\eta_{el_{CHP}}}{\eta_{th_{CHP}}} + \frac{1}{COP_{HP2}}\right)\right)^{-1} \cong p_{gas} \cdot 1.64 \tag{22}$$

$$p_6 = \frac{p_{gas}}{\eta_{el_{CHP}}} \cong p_{gas} \cdot 2.12 \tag{23}$$

$$p_7 = p_{gas} \cdot \frac{COP_{HP1}}{\eta_{GB}} \cong p_{gas} \cdot 3.03 \tag{24}$$

$$p_8 = p_{gas} \cdot \frac{COP_{HP1}}{\eta_{GB}} \cong p_{gas} \cdot 3.41 \tag{25}$$

Table 2 defines nine scenarios, the algorithm schematized by the flowchart in Figure 5 allocates for each scenario σ the residual thermal load (i.e., the heat demand subtracted by the heat output of the storage units defined by the preliminary optimization of the unit commitment) to the five generator technologies in place in Canavese.

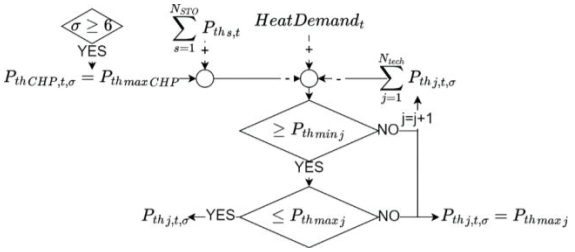

Figure 5: Algorithm for the load allocation to the j-th technology at time interval t and scenario σ

https://doi.org/10.52202/077185-0212

Once the residual thermal output is allocated for each time interval and scenario among the technologies, it is assessed the electrical output associated through Equation (26)

$$P_{el_{j,t,\sigma}} = \left(\alpha_{el_j} + \beta_{el_j} \cdot \frac{P_{th_{j,t,\sigma}}}{N_j}\right) \cdot N_j \tag{26}$$

Then, market bids must be formulated such that the summation of $P_{el_{j,t,\sigma}}$ for each technology is equal to the MES injection/withdrawal program for any market clearing price. More in detail, nine bid couples with the quantity defined in Eq. (28, 29) should be presented, where it is worth noting that since it is considered a market with hourly resolution, the factor converting electric production [MW] to the quantity offered [MWh] is 1. The price associated to the bid is defined by Eq. (30, 31); in case of σ=8, $p_{t,\sigma_{BID}}$ is set to the market cap price. "OFF" and "BID" define the purposes of sell and buy electricity, respectively.

$$Q_{t,\sigma_{required}} = \sum_{j=1}^{N_{tech}} P_{el_{j,t,\sigma}} \tag{27}$$

$$Q_{t,\sigma_{BID}} = \begin{cases} \sum_{j=1}^{N_{tech}} P_{el_{j,t,\sigma}} - \sum_{\omega=\sigma+1}^{8} Q_{t,\omega_{required}}, & Q_{t,\sigma_{required}} < 0 \\ 0, & Q_{t,\sigma_{required}} \geq 0 \end{cases} \tag{28}$$

$$Q_{t,\sigma_{OFF}} = \begin{cases} 0, & Q_{t,\sigma_{required}} \leq 0 \\ \sum_{j=1}^{N_{tech}} P_{el_{j,t,\sigma}} - \sum_{\omega=0}^{\sigma-1} Q_{t,\omega_{required}}, & Q_{t,\sigma_{required}} > 0 \end{cases} \tag{29}$$

$$p_{t,\sigma_{BID}} = p_{\sigma+1} \tag{30}$$

$$p_{t,\sigma_{OFF}} = p_{\sigma} \tag{31}$$

This strategy allows that the required quantity $Q_{t,\sigma_{required}}$ is allocated in market whatever scenario will be defined by the cleared p_{el_t}.

3.3 Redispatch optimization

The last step happens after the market clearing, that sets up the accepted bids among those presented by the MES manager, uniquely defining $P_{el_{program_t}}$ injection/withdrawal program for any time interval t.

An optimization problem is solved analogously to that described in Section 3.1. The only differences rely in the objective function reformulated as in Eq. (32) without the cost of electricity consumption. Indeed, the electricity output is fixed, and this cost cannot be varied acting on the optimization variable.

$$\min_{\overrightarrow{P_{th}}} \sum_{t}^{H} \sum_{i}^{N_{units}} \left(C_{gas_{i,t}} + C_{O\&Mvar_{i,t}} + C_{SU_{i,t}}\right) \tag{32}$$

Moreover, to guarantee the compliance to this requirement the following constraint is added.

$$\sum_{i=1}^{N_{units}} P_{el_{i,t}} = P_{el_{program_t}} \quad \forall \, t \leq H \tag{33}$$

4 THE IMPACT OF UNCERTANTIES

This section focuses on the uncertainties impact quantification, for this purpose the optimizer described in Section 3.1 is executed with a first series of hourly data assumed as forecast for electricity price and heat demand. Then a set of bids is defined according to the methodology presented in the Section 3.2, these bids are accepted or rejected according to the market clearing price (i.e., a new time series that stochastically deviates from the first values). This defines a program of electricity withdrawal/injection that must be respected by the MES. Assuming this program, the imposed electricity clearing price, and a time series for the actual heat demand (that deviates from the forecasted values analogously to the electricity price), the redispatch optimization, as described in Section 3.3 is performed.

https://doi.org/10.52202/077185-0212

4.1 Modelling the uncertainty

To capture electricity price and heat demand uncertainty in forecasts, it is crucial to focus on the probable error at each time interval, representing the spread of actual values around predicted ones. Common metrics usually adopted in the literature are MAPE, MSE, and MAE [21]. However, for the purpose of this paper is preferable to model the probability density function of the forecast error. This is done through a normal distribution characterized by the mean, i.e., the forecasted value, and the normalized standard deviation $\hat{\sigma}$, i.e., the ratio of standard deviation to mean and linearly correlates with typical error metrics [22], $\hat{\sigma}$=0.1 corresponds to 7.98 MAPE.

Finally, it should be considered that the error is usually autocorrelated [23] showing a persistence. Indeed, if the error at time t, ϵ_t, is relevant and positive, it is hardly probable that at time t+1 it will swing to the opposite lower limit. Instead, there is a tendency for errors to persist in the same direction or exhibit gradual changes over time. For this purpose, the persistency p is defined as the maximum difference between relative errors at two consecutive time intervals normalize on $\hat{\sigma}$.

$$p = \frac{\left(\frac{\epsilon_{t+1}}{x_{t+1}} - \frac{\epsilon_t}{x_t}\right)_{max}}{\hat{\sigma}} \tag{34}$$

Henceforth, $\hat{\sigma}$ and p are used with the subscripts "ZP" and "HD" relative to the electricity zonal price and heat demand respectively. For the purpose of this investigation, p_{ZP} and p_{HD} are assumed to 0.2.

4.2 Impact quantification

This subsection investigates the impact of $\hat{\sigma}_{PZ}$ and $\hat{\sigma}_{HD}$ in the range 0 to 1 simulating the preliminary unit commitment optimization, the bidding and the redispatch of the modelled MES for one winter week. For the forecasted data real-data already employed in [14] are assumed. Figure 6, generated with 500 samples, shows the boxplot chart of ΔCost (i.e., the difference between actual cost, after the redispatch optimization, and the forecasted cost according to the first attempt unit commitment optimization). Figure 6(a) and (b) show the impact of $\hat{\sigma}_{PZ}$ and $\hat{\sigma}_{HD}$ respectively while the other parameter is kept to 0. Median and quartiles values are then fitted with quadratic curves.

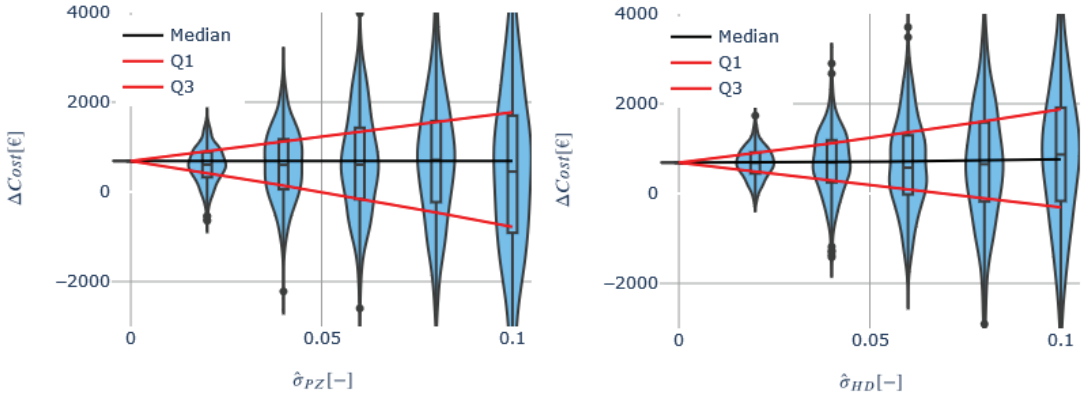

(a) (b)

Figure 6: electricity price (a) and heat demand (b) uncertainty impact on actual costs

It is possible to appreciate that as the input parameter uncertainty increases it is reflected in an actual cost uncertainty. It is interesting to observe that the cost may be lower than estimated, indeed an electricity price lower than expected lead to a cheaper provision of primary energy reflected in a considerable saving. Analogously if the real heat demand is lower than forecasted, alongside an optimal redispatch of storages, the usage of gas boilers, that are independent on the electricity carrier constrained to the market program, can be reduced, leading to a gas and money saving.

It is also worth observing that as $\hat{\sigma}$ goes to zero, the dispersion of costs goes to zero as well, even if the absolute value of ΔCost remains positive: 689 € corresponding to 3.14% of the week costs. This is due to an intrinsic approximation of the adopted bids definition. Indeed, in eq. (18-25) rough efficiency values are adopted but real values depend on the generators load that it is not known *a priori*, thus in the neighborhood of values $p_{1\text{-}8}$, the bidding strategy may result slightly suboptimal.

https://doi.org/10.52202/077185-0212

However, it can generally be appreciated how the expected final cost is quite robust respect to the investigated uncertainties. The median values of cost difference distribution represent the most probable value and is therefore assumed as the main indicator of the uncertainty cost. Through a 2nd degree polynomial function, the tendency of the median ΔCost versus the combined effect of $\hat{\sigma}_{PZ}$ and $\hat{\sigma}_{HD}$ has been fitted (black line in Figure 6). The impact of $\hat{\sigma}_{PZ}$ its negligible; while the dependency on $\hat{\sigma}_{HD}$ is almost linear showing a growth of approximatively 0.62 percentage point of cost uncertainty for a 0.1 increment in $\hat{\sigma}_{HD}$, it is equivalent to a growth by 0.08% in expected operational cost per heat demand forecast MAPE percentage point. These results demonstrate the effectiveness of the proposed algorithm for bids definition and the subsequent redispatch optimization.

5 STOCHASTIC APPROACH IMPLEMENTATION

The previous section demonstrated that the methodology proposed is in the Section 3 is robust with respect of the electricity price and slightly impacted by the heat demand forecast uncertainty. However, the robustness could be further enhanced by adopting stochastic methodologies as well that one presented in this Section.

The problem consists in minimizing the expected value of a function under the uncertainty of some parameters. Figure 7 exemplifies the concept for a problem with only one optimization variable, *x*, and one uncertain parameter *k*. The assumed case study problem has 360 free optimization variables (the hourly thermal output of the ten generators and storages) and 72 uncertain parameters (the hourly electricity price and heat demand).

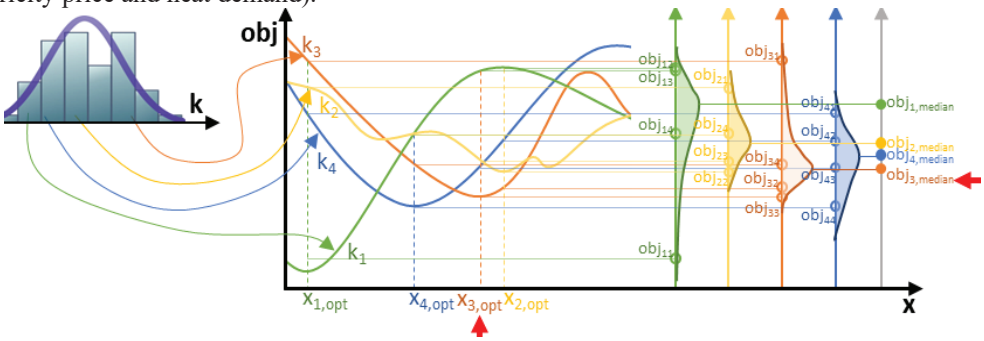

Figure 7: Stochastic methodology to minimize the expected *obj* value under the uncertainty of k.

The proposed randomized approach involves the stochastic selection of a set of *k* parameter values from the known probability distribution. Then it performs a deterministic optimization, in order to determine for each k_i an optimal value of *x*, $x_{i\ opt}$. At this point, the objective function is calculated, in $x_{i\ opt}$, for all other values of *k* present in the initially sorted set to estimate the probability distribution of the objective function. The probability distributions can then be evaluated according to different metrics, that prefer minimization at a higher risk or vice versa. The main proposed indicator to evaluate the obtained distribution is the median value. So, the $x_{i\ opt}$ whose associated cost distribution has the lowest median value is selected as the optimal robust solution. The example reported in Figure 7 has only four values in the set of *k*, to increase the effectiveness of the presented methodology larger sets must be adopted.

Considering the median value as the main indicator, the authors integrated the presented stochastic approach in the uncertainty range investigated in the previous section, concluding that the lowest expected cost is obtained for the same solution when applying the scenario approach presented in Section 3. Nevertheless, if the MES operator looks at a more conservative strategy and assesses the probability distribution of costs at percentiles beyond 75, the proposed stochastic methodology reduces the worst-case cost up by 0.3% if compared to the scenario approach introduced in Section 3.

6 CONCLUSION

This paper addressed the problem of scheduling optimization of a Multi-Energy System under the electricity price and local energy demand uncertainty. Two methodologies were introduced, the first relies in an algorithm to transpose the preliminary scheduling, obtained through standard mathematical

https://doi.org/10.52202/077185-0212

programming algorithms, into a set of bids to be submitted in the electricity market. The second integrates this procedure into a stochastic iteration.

A preliminary unit commitment optimization problem is solved to obtain a first attempt guess of the best storages scheduling; then the residual load, that must be provided to meet the local energy demand, is allocated among the different generators figuring out as many price scenarios as many possible generators cost merit order can be listed. The algorithm presented in Section 3.2 defines a set of bids each characterized by a quantity and a price so that whatever is the market clearing price it is ensured that the MES injection/withdrawal program to/from the electricity grid is such to satisfy the local energy demand as close as possible to the lowest cost. Defined the program to which be constrained, a redispatch optimization is carried out approaching the real time for a fine tuning of the unit commitment in light of short term forecast whose uncertainty is negligible.

However, the proposed approach performs the storage scheduling guess based on uncertain forecasted values, then the residual load is allocated considering fixed rough values of efficiency. So final costs may result higher than the minimum possible. Nevertheless, considering the Canavese plant, connected to the Milan DHN, the impact of electricity price and heat demand uncertainties is investigated concluding that the electricity price forecast error has a negligible impact and even the heat demand has a reduced influence. For each MAPE percentage point of the heat demand forecast, over a 48-hour horizon, it is observed that the expected cost of operating the MES increases by 0.08 percent.

Moreover, when this approach is integrated in the stochastic methodology for robust optimization, presented in Section 5, no appreciable improvement was observed. This demonstrates the intrinsic robustness of the MES when equipped with large storage, able to mitigate the heat demand uncertainty, and the effectiveness of the presented bidding methodology to guarantee the supply of the demand, the compliance to the grid interaction program defined by the market at a low cost under the uncertainty of electricity price forecast. However, the randomized methodology allows to assess the probability distribution of operating costs in depth and selecting better operating and bidding strategy according to more conservative attitude that wants to minimize costs at the third quartile or in worse cases.

The presented methodology, even if applied to the case study introduced in the Section 2, has been developed generally for MESs under operational parameters uncertainties and can be adopted for further investigations considering multiple markets (e.g., intraday electricity markets, spot gas markets), sensitivity to storage size, the possible time-shift in parameters, the peaks and the uncertainty of local RES generation (e.g., from solar thermal collector) covering a load fraction.

NOMENCLATURE

Abbreviations and Acronyms

CHP	Cogenerative gas-fired gas engines
COP	Coefficient of Performance
DHN	District Heating Network
EB	Electric Boiler
GB	Gas Boiler
HP	Heat Pumps
MES	Multi-Energy System
STO	Thermal energy storage
SU	Start-Up

Variables

C	Cost (€)
E	Energy ((MWh)
H	time intervals in the optimization horizon
N	number (–)
P	power (MW)
p	price (€/MWh), error persistency (-)
Q	bid quantity (MWh)
y	binary variable (-)
α	Carrier x power regressor (MW_x)
β	Carrier x power regressor (MW_x/MW_{th})
η	efficiency (-)
σ	market clearing scenario number (#)
$\hat{\sigma}$	Error normalized standard deviation (-)

Subscript

0	initial
BID	purpose of buying electricity
ch	charge
disch	discharge
el	electrical
gas	natural gas
HD	Heat Demand
i	unit index
j	technology index
n	day of optimization index
OFF	purpose of selling electricity

https://doi.org/10.52202/077185-0212

s	storage index	x	generic carrier
t	time interval index	ZP	Zonal Price
th	thermal		

REFERENCES

[1] Mancarella P. MES (multi-energy systems): An overview of concepts and evaluation models. Energy 2014;65:1–17. https://doi.org/https://doi.org/10.1016/j.energy.2013.10.041.

[2] Bartolini A, Carducci F, Muñoz CB, Comodi G. Energy storage and multi energy systems in local energy communities with high renewable energy penetration. Renew Energy 2020;159:595–609. https://doi.org/https://doi.org/10.1016/j.renene.2020.05.131.

[3] Gabrielli P, Poluzzi A, Kramer GJ, Spiers C, Mazzotti M, Gazzani M. Seasonal energy storage for zero-emissions multi-energy systems via underground hydrogen storage. Renewable and Sustainable Energy Reviews 2020;121:109629. https://doi.org/https://doi.org/10.1016/j.rser.2019.109629.

[4] Ramsebner J, Haas R, Ajanovic A, Wietschel M. The sector coupling concept: A critical review. WIREs Energy and Environment 2021;10:e396. https://doi.org/https://doi.org/10.1002/wene.396.

[5] Gray N, McDonagh S, O'Shea R, Smyth B, Murphy JD. Decarbonising ships, planes and trucks: An analysis of suitable low-carbon fuels for the maritime, aviation and haulage sectors. Advances in Applied Energy 2021;1:100008. https://doi.org/https://doi.org/10.1016/j.adapen.2021.100008.

[6] Ikäheimo J, Kiviluoma J, Weiss R, Holttinen H. Power-to-ammonia in future North European 100 % renewable power and heat system. Int J Hydrogen Energy 2018;43:17295–308. https://doi.org/https://doi.org/10.1016/j.ijhydene.2018.06.121.

[7] Rivarolo M, Riveros-Godoy G, Magistri L, Massardo AF. Clean hydrogen and ammonia synthesis in paraguay from the Itaipu 14 GW hydroelectric plant. ChemEngineering 2019;3:1–11. https://doi.org/10.3390/chemengineering3040087.

[8] Vignali R, Falsone A, Ruiz F, Gruosso G. Towards a comprehensive framework for V2G optimal operation in presence of uncertainty. Sustainable Energy, Grids and Networks 2022;31:100740. https://doi.org/https://doi.org/10.1016/j.segan.2022.100740.

[9] Bianchi F, Falsone A, Vignali R. Vehicle-to-Grid and ancillary services: a profitability analysis under uncertainty*. IFAC-PapersOnLine 2023;56:7077–83. https://doi.org/https://doi.org/10.1016/j.ifacol.2023.10.571.

[10] Renewables 2023. Paris: 2024.

[11] Vannoni A, Sorce A, Traverso A, Fausto Massardo A. Techno-economic optimization of high-temperature heat pumps for waste heat recovery. Energy Convers Manag 2023;290. https://doi.org/10.1016/j.enconman.2023.117194.

[12] Vannoni A, Sorce A, Traverso A, Massardo AF. Large Size Heat Pumps Advanced Cost Functions Introducing the Impact of Design Cop on Capital Costs. SSRN 2023. https://doi.org/10.2139/ssrn.4376419.

[13] Lund H, Werner S, Wiltshire R, Svendsen S, Eric J, Hvelplund F, et al. 4th Generation District Heating (4GDH) Integrating smart thermal grids into future sustainable energy systems. Energy 2014;68:1–11. https://doi.org/10.1016/j.energy.2014.02.089.

[14] Corsetti E, Riaz S, Riello M, Mancarella P. Modelling and deploying multi-energy flexibility: The energy lattice framework. Advances in Applied Energy 2021;2. https://doi.org/10.1016/j.adapen.2021.100030.

[15] Zeng Q, Fang J, Chen Z, Conejo AJ. A two-stage stochastic programming approach for operating multi-energy systems. 2017 IEEE Conference on Energy Internet and Energy System Integration (EI2), 2017, p. 1–6. https://doi.org/10.1109/EI2.2017.8245587.

[16] Blanco I, Guericke D, Andersen AN, Madsen H. Operational planning and bidding for district heating systems with uncertain renewable energy production. Energies (Basel) 2018;11. https://doi.org/10.3390/en11123310.

[17] Castelli AF, Moretti L, Manzolini G, Martelli E. Robust optimization of seasonal, day-ahead and real time operation of aggregated energy systems. International Journal of Electrical Power and Energy Systems 2023;152. https://doi.org/10.1016/j.ijepes.2023.109190.

[18] Technology Data-Energy Plants for Electricity and District heating generation - Data sheet for Electricity and district heat production - Updated February 2024. Danish Energy Agency: 2024.

[19] Technology Data-Energy storage –Datasheet for energy storage – Updated September 2023. 2023.

[20] Satyavada H, Baldi S. A novel modelling approach for condensing boilers based on hybrid dynamical systems. Machines 2016;4. https://doi.org/10.3390/machines4020010.

[21] Pavićević M, Popović T. Forecasting Day-Ahead Electricity Metrics with Artificial Neural Networks. Sensors 2022;22. https://doi.org/10.3390/s22031051.

[22] Feron B, Monti A. A Market-Based Optimization Approach for Domestic Thermal and Electricity Energy Management System: Formulation and Assessment. Information 2018;9. https://doi.org/10.3390/info9050120.

[23] Kontogiannis D, Bargiotas D, Daskalopulu A, Arvanitidis AI, Tsoukalas LH. Error Compensation Enhanced Day-Ahead Electricity Price Forecasting. Energies (Basel) 2022;15. https://doi.org/10.3390/en15041466.

ACKNOWLEDGEMENT

This work has been financed by European Union under contract n.101075731 – SENERGY NETS.

 https://doi.org/10.52202/077185-0212